Silica-aerogel thermal expansion induced by submonolayer helium adsorption

P. Thibault, J. J. Préjean, and L. Puech
Centre de Recherche sur les Très Basses Températures-CNRS, associé à l'Université Joseph Fourier, Boîte Postale 166, 38042 Grenoble-Cédex 9, France
(Received 5 June 1995)

We present measurements of the thermal expansion of silica-aerogels of various densities in the two following situations: thermal expansion of evacuated samples and the additional expansion due to ^{4}He adsorption on the silica surface in the temperature range 2–80 K. At the same time we measured the number of ^{4}He atoms adsorbed at the surface. To analyze the adsorption data we use a Brunauer-Emmett-Teller model, where we introduce a distribution of binding energies to take into account the surface heterogeneity. A simple model, involving the same distribution, allows us to relate the expansion to adsorption. We therefore determine some microscopic parameters for the adsorption energies and derive the elastic properties at different scales of the fractal structure.

I. INTRODUCTION

The adsorption-induced expansion of porous media[1] has long been observed for both inert gases and more polarizable species like the adsorption of water on charcoal,[2] and more recently for its influence on the light emission spectrum by porous silicon.[3] The case of silica-aerogels is complex, because of both (i) its very poorly characterized surface energies, and (ii) its very complex geometry. Adsorption decreases the surface tension and therefore tends to increase the specific area, inducing an expansion. For aerogels the latter effect, which originates from mechanisms at microscopic scales, cannot be related simply to the macroscopic elastic constants. The macroscopic elastic constants are measured by the macroscopic deformation under external stress. In particular, the Young modulus E is found experimentally[4] to be much smaller than that of pure amorphous silica ($E_{SiO_2}=1$ Mbar) normalized by the density ratio ρ/ρ_{SiO_2}. For instance, for neutral-reacted aerogels of density $\rho<0.4$ g/cm^3, a scaling relation[4] has been established for $E(\rho):E(\text{Mbar})\approx 1.3(\rho/\rho_{SiO_2})^{3.8}$. For the aerogel presented here ($\rho=0.16$ g/cm^3, where $\rho_{SiO_2}=2.2$ g/cm^3) we calculate $E\approx 60$ bar, i.e., 10^3 times smaller than $E_{SiO_2}(\rho/\rho_{SiO_2})=7\times 10^4$ bar. Such a small value of E can be attributed to two mechanisms. One mechanism, occurring at intermediate scales,[5,6] is due to the bending of the microrods that constitute the porous structure. The other, at a microscopic scale, comes from the compression of the particles of silica which compose the microrods. Because of the former mechanism, the latter strain might be far less than the macroscopically imposed strain. On the other hand, strains of microscopic origin (thermal expansion, adsorption, etc.) induce a macroscopic strain of the same order. Thus if v denotes the volume of the individual silica particles and V that of the whole gel, we have to distinguish between

$$\varepsilon=\left[\frac{V\partial v}{v\partial V}\right]_{\text{external stress}}\ll 1\ ,$$

when the deformation is due to stresses applied at macroscopic scales and $(V\partial v/v\partial V)_{\text{internal stress}}\approx 1$, when the deformation is due to microscopic stresses.

The final goal of our study is to estimate the value of ε. For this purpose, we have measured simultaneously the adsorbed fraction n_{ads} of He gas and the expansion dV/V of the porous medium. Because of the spreading pressure the adsorption induces a deformation ds/s of the local surface, which is transmitted to the macroscopic scales. The quantity n_{ads} is related to the van der Waals potential Δ_1 at the surface. In this paper, we show that the temperature dependence of n_{ads} can be understood if one assumes a broad distribution of binding energies Δ_1 on the silica surface. We show that we can estimate the value of ds/s, and consequently of ε, by using a simple model and the distribution of Δ_1. The paper is organized as follows. In Sec. I, we describe the cell that we have built to measure the linear expansion of gels without any external stress. Also, we show the necessity of taking special precautions in order to avoid the effects of the two following physical properties: (i) the very low thermal diffusion in the measurement of the expansion of dry aerogels, and (ii) the slow thermally activated diffusion of gas atoms from outer to inner parts of the porous structure in adsorption experiments. Section II is devoted to an experimental study of the adsorption, and to the modified Brunauer-Emmett-Teller (BET) model introduced to account for the results. In Sec. III, we show that the expansion of the gel is directly related to the binding energies of the He atoms on the gel surface. We also deduce the ratio ε between the microscopic and macroscopic strain of the gel under macroscopic stress.

0163-1829/95/52(24)/17491(10)/$06.00

II. EXPERIMENTAL PROCEDURE

A. Samples

The study of the expansion induced by adsorption has been performed on a neutrally reacted aerogel of density $\rho=0.16$ g/cm^3. It is one of a batch of samples prepared by Forêt and Woignier from the Laboratoire de Science des Matériaux Vitreux in Montpellier[7] with densities in the range $\rho=0.08$ to 0.36 g cm^{-3}. In Sec. IV, we present measurements of their thermal expansion when evacuated. The chemical preparation gives a tiny structure of meshes with small constitutive elements of interconnected silica particles of a few tens of atoms.

B. Dilatometer

The uniaxial length change of silica aerogels is capacitively measured by a differential dilatometer shown in Fig. 1. The sample of typical volume $V=0.5\times0.5\times0.8$ cm^3 lies on a flat copper holder, and an articulated plate rests upon its top. The electrodes (of surface 1 cm^2) are made of a thin copper film deposited onto a kapton foil. Two electrodes (a) and (b) are glued onto the fixed upper part of the dilatometer, the third one (c) is glued onto the articulated plate (see Fig. 1). Each of the two capacitors, labeled C_x [electrodes (a) and (c)] and C_r [electrodes (b) and (c)] have a gap of about 100 μm. A relative expansion of the sample with respect to the cell induces a change in the electrode spacings and therefore in the capacitor ratio C_x/C_r. The capacitances are about 10 pF, and the use of a standard capacitive bridge[8] provides a 5×10^{-7} resolution on the ratio C_x/C_r. With a sensitivity of $(dC/CdL)=5\times10^{-3}/\mu$m, the corresponding length change resolution is $dL\approx1$ Å or $dL/L\approx10^{-8}$. All the apparatus being made out of copper, the absolute length change is obtained after correction from copper expansion, which is very regular and well known[9] over that temperature range. Nevertheless, we measured small deviations for a copper sample, which ideally should give $dC=0$, but which proved to be 10^{-3} of the total copper thermal expansion on the full temperature range between 4 and 80 K. As we do not know the exact origin of this shift, the latter is taken into account in our error bars. The advantages of such a dilatometer are that we are not obliged to glue the porous sample, and that there is virtually no weight pressing on it. Thus we are able to measure the expansion of a gel free of external stress, which is very important as these materials offer very low bulk modulii. As a drawback, the system becomes very sensitive to any external vibration, which was the principal factor limiting our experimental resolution.

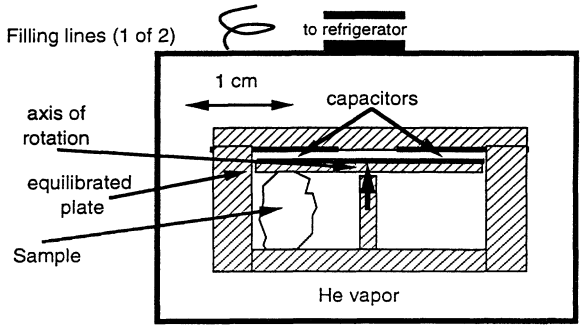

FIG. 1. Schematic view of the dilatometer.

C. Experimental procedures

Before any measurement, the cell containing the sample is evacuated for 48 h from residual gases in a 10^{-6} torr vacuum at 320 K in order to avoid spurious data, as was stressed in Ref. 6. Then the sample is cooled down and, for measurements of the expansion of dry gel, we start the run at 80 K. The temperature is slowly decreased down to 2 K and then back. The thermal conductivity of aerogels is very low at these temperatures; Thus we performed each sweep in about 24 h. However, we still observed a small hysteresis between decreasing and increasing temperature. Assuming a single (temperature-dependent) thermal diffusion time for heat through the sample, we average properly the data at increasing and decreasing T. We checked that, after this correction, data obtained at different temperature sweep rates $\partial T/\partial t$ fall on the same curve, which is assumed to be the $\partial T/\partial t\rightarrow0$ limit. In the adsorption study, we noted the great advantage of the simultaneous measurement of pressure (i.e., the nonadsorbed fraction at given T), and of length change dL when it is compared to a single isotherm adsorption measurement. Indeed, at the lowest temperatures, fixing T and adding ^{4}He lead to nonreproducible results upon expansion. In fact, it is much better to start at high T (above 35 K in our case) and to slowly decrease the temperature. We interpret this as a manifestation of the very slow thermally activated diffusion of atoms from outer to inner parts of the gel.

D. Measurements of the quantity of adsorbed gas

We introduce a quantity $n_{\rm tot}$ of gas in the cell of volume $V_{\rm cell}$. In the hypothesis of a perfect gas, the quantity $n_{\rm ads}$ of adsorbed gas is given by the measurement of the pressure P:

$$P=n_{\rm gas}\frac{RT}{V_{\rm cell}}=(n_{\rm tot}-n_{\rm ads})\frac{RT}{V_{\rm cell}}\ . \tag{1}$$

Some precautions have to be taken. First we optimized the experimental setup to reduce the dead volumes and to enhance the sample to cell surface ratio (about 20 m^2/100 cm^2). Two capillaries (1.5-mm diameter, 120 cm long) join the cell to the top of the cryostat. One is used to introduce a given quantity of He atoms, the other one is for the measurement of the pressure. We correct the value of $V_{\rm cell}$ in Eq. (1), taking the low-temperature cell volume plus the contribution $VT/300$ K of the dead volume V (86 cm^3) at room temperature, plus the contribution of the capillaries. In the latter case we assume a constant temperature gradient along the capillaries between T and

300 K. The pressure is measured with a mks baratron located at room temperature (relative precision of 0.1%, resolution ≥ 0.02 torr). To obtain the value of the pressure in the cell, we correct[10] the data from the thermomolecular pressure drop due to the capillary joining cold and room-temperature parts. Nevertheless, the impreciseness of our pressure measurement is enhanced in the two following cases. For very low pressures (i.e., for a high adsorption rate), our resolution limited to 10^{-2} torr is not sufficient. For small adsorption rates, P is close to the calculated value $n_{\text{tot}}RT/V_{\text{cell}}$: the difficulty is to resolve with enough accuracy the minute change in the absolute value of the pressure caused by the adsorbed atoms.

III. ADSORPTION STUDY

A. Introduction

In this section we focus on adsorption of ^{4}He atoms at the gel surface, and we correlate it to the observed length changes in Sec. IV. The adsorption is related to the van der Waals binding energy Δ_1 on one silica surface. In general, one assumes a single value of Δ_1 to analyze adsorption data in order to measure the specific area of porous media. The latter proved to be very large[11] in the case of aerogels (~ 700 m^2/g of the sample). Owing to the tortuous surface of aerogels, one can expect the existence of a distribution $P(\Delta_1)$ of Δ_1. The goal of this section is to characterize accurately the surface by determining both the number of adsorption sites n_{sites} and the potential distribution $P(\Delta_1)$. It requires experiments to be performed under very well controlled conditions, as already explained in Sec. II C.

B. Experimental data

We present our pressure measurements $P_{\text{meas}}(T)$ in the two following diagrams. First, in Fig. 2(a), we have plotted $n_{\text{ads}}/n_{\text{tot}}$ vs T, where the quantity $n_{\text{ads}}/n_{\text{tot}}$ is calculated from Eq. (1): $n_{\text{ads}}/n_{\text{tot}}=1-P_{\text{meas}}/P_{\text{tot}}$. Here P_{tot} denotes the pressure which should exist in the absence of adsorption: $P_{\text{tot}}=n_{\text{tot}}RT/V_{\text{cell}}$. The different curves correspond to different amounts n_{tot} of ^{4}He atoms initially introduced in the cell. [See the legend of Fig. 2(a).] The fraction $n_{\text{ads}}/n_{\text{tot}}$ tends to 0 at high enough temperature. We note that, when the value of P_{meas} is close to that of

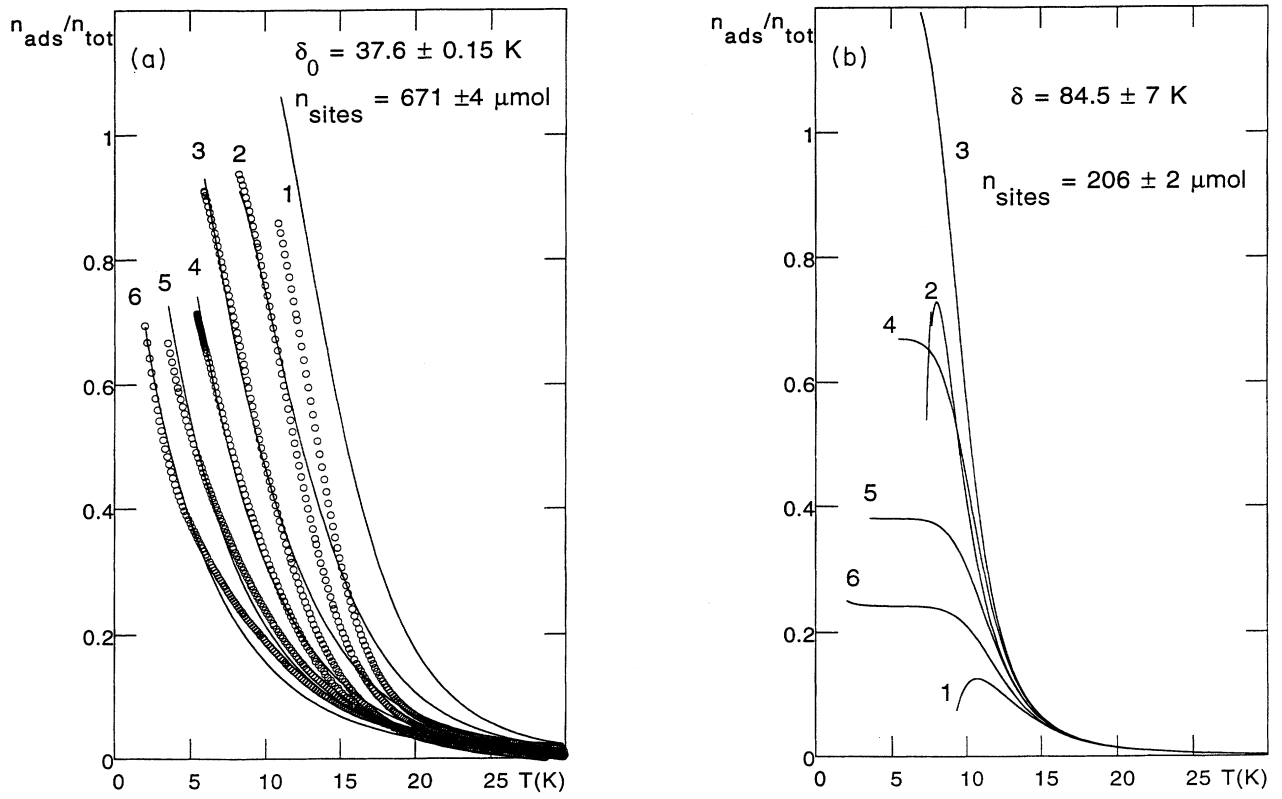

FIG. 2. (a) Temperature dependence of the ratio of the number n_{ads} of He-adsorbed atoms to the total number n_{tot} of atoms introduced in the cell. The density ρ of the aerogel equals 0.16g/cm^3. Each curve corresponds to a different value of n_{tot}: 21.81 μmol (1), 64.32 μmol (2), 164.4 μmol (3), 307.7 μmol (4), 541.5 μmol (5), and 854 μmol (6). (b) Result of the best fit to the data shown in (a) when one assumes a single value of $\delta=\Delta_1-\Delta$.

P_{tot}, a value of n_{tot} slightly underevaluated (giving an underevaluated value of P_{tot}), or the uncertainty on the measurement of P_{meas} can lead to negative values of the quantity n_{ads}/n_{tot}. On the other hand, when P_{meas} is very small, the calculation of $n_{ads}(T,P)$ from the model presented below using $P=P_{meas}$ may give $n_{ads}>n_{tot}$. To avoid these problems, we prefer to present our data in the P_{meas}/P_0 vs T diagram of Fig. 3. P_{meas}/P_0 will be compared directly with the pressure calculated from our model, without explicit reference to P_{meas} for calculating $n_{ads}(T,n_{tot},V_{cell})$. The quantity $P_0(T)$ is defined below [see Eq. (3)].

C. Interpretation

A first remark concerns the width in binding energies involved in our experimental data. In a simple BET (Ref. 12) model, there are only two binding energies, one Δ_1 between the first-layer atoms and the substrate, and another Δ characterizing the binding energy for the liquid above ($\Delta\approx 10$ K in case of helium). With such a model, when decreasing the temperature, the adsorbed fraction exhibits a very rapid variation at some temperature T_1 followed by a saturation. The temperature T_1 depends on Δ_1 and n_{tot}. In our case, the number of adsorbed atoms varies smoothly with the temperature, which indicates the existence of many binding energies. We therefore introduce a distribution in Δ_1. We will discuss the two attempts we have made, because of their physical origin. We first considered a normalized "stripe" of equiprobable energies between Δ and Δ_{max}. This stripe is associated with a total number of adsorbing sites n_{sites}. We finally found that three of these stripes were necessary to reasonably reproduce our experimental data. In order to lower the number of parameters (three numbers of sites and three upper binding energies Δ_{max}), we also made this calculation with an exponential distribution, involving only two parameters.

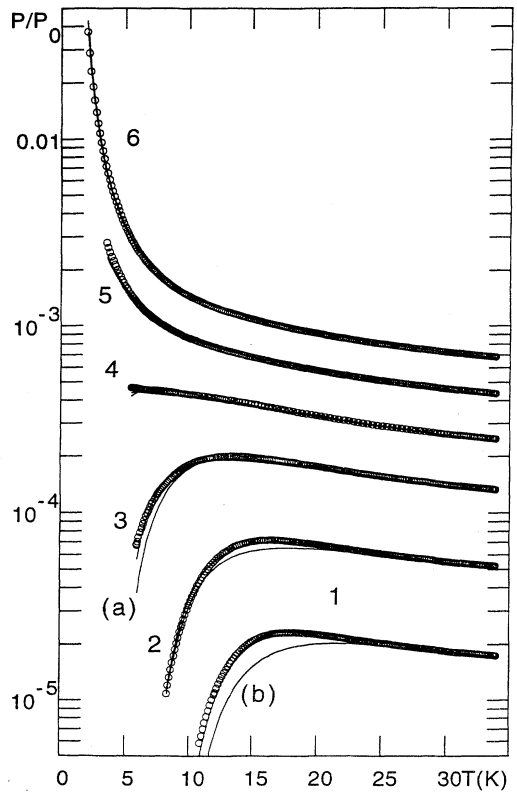

FIG. 3. The temperature dependence of the measured pressure normalized to the saturated pressure $P_0(T)$ is presented in a semilog diagram. The points represent the experimental data, the solid curves correspond to the fits involving a distribution $P(\Delta_1)$ of the binding energy Δ_1. See text.

To elaborate, first we summarize some results, important in our study, of the original BET model. We introduced the BET model through the grand partition function ξ and the grand potential $\Omega_{/site}=-kT\ln(\xi)$ per site:

$$\xi=1+\exp[B(\Delta_1+\mu)](\Sigma x^n)=1+\frac{cx}{1-x}\ , \tag{2}$$

where $c=\exp(\beta\delta)$, with $\delta=(\Delta_1-\Delta)>0$, and where $x=\exp\beta(\Delta+\mu)$. Here μ denotes the chemical potential for helium atoms. The quantity x is the ratio of the pressure P to the saturating pressure $P_0(T)$,

$$x=\frac{P}{P_0(T)},\quad P_0=\frac{RT}{V_L}\exp(-\Delta/T)\ , \tag{3}$$

where V_L is the molar volume of the liquid. In this basic model, each site is assumed to be independent of the others. The derivative of $\Omega_{/site}$ with respect to μ provides the mean number $\bar{n}$ of atoms of He in a column above the site. We can write $\bar{n}$ as the sum of the number $\bar{n}_1=(\xi-1)/\xi$ of the He atoms adsorbed on the silica surface in the first layer plus the number $\bar{n}_L$ of atoms in the other "liquidlike" layers:

$$\bar{n}=\bar{n}_1+\bar{n}_L,\quad \bar{n}_1=\frac{cx}{1-x+cx},\quad \bar{n}_L=\bar{n}_1\frac{x}{1-x}\ . \tag{4}$$

The total number of adsorbed atoms n_{ads} is given by Eq. (4), and the number of sites is $n_{ads}=\bar{n}n_{sites}=\bar{n}_1 n_{sites}/(1-x)$. Using the experimental values of x and a *single* value of Δ_1, we fit all the data shown in Fig. 2(a). The best fit, which gives $\delta\approx 85$ K, provides shapes of the curves $n_{ads}/n_{tot}(T)$ which are very different from those given by experiment, as shown in Fig. 2(b). For a given value of n_{tot}, the calculated curve varies much more rapidly with T than the experimental data, and it saturates at low temperatures in contrast to our measurements. Thus we are obliged to suppose the existence of a broad distribution of Δ_1. In the following, we will average any quantity involving Δ_1 (i.e., δ) over its distribution $P(\delta)$, which is the major improvement to the standard use of the BET calculation. In general, there exist no analytical solutions, so we have to integrate the different quantities over $P(\delta)$ numerically. In the Appendix, we give details about the way of carrying out such integrations for the two distributions that we have tried.

For n_{ads}, we have to calculate

$$n_{ads}(x)=n_{sites}\int_0^{\delta_{max}}\bar{n}(\delta,x)P(\delta)d\delta\ . \quad (5)$$

Here $\int P(\delta)d\delta=1$. Equation (1) can be rewritten

$$x=p_{eff}\left[1-\frac{n_{ads}(x)}{n_{tot}}\right], \quad (6)$$

where $p_{eff}=(V_L/V_{cell})\exp(\beta\Delta)$ is the value of x in the absence of adsorption, and n_{ads} is given by Eq. (5). The two parameters V_L ($=27$ cm^3) and Δ ($=10.6$ K) necessary to calculate P_0 are known. Δ has been chosen to fit approximately the vapor pressure around 4 K. The other parameters (T,V_{cell},n_{tot}) are fixed by the experiment. Once a distribution $P(\delta)$ is imposed, one can calculate $x(T)$ from Eq. (6). So we have to choose a distribution which can account for the shape of the experimental curve $x_{expt}(T)$ deduced from the measured pressure P_{meas} (see Fig. 3). Our method consists of fitting all the x_{expt} data altogether to determine the values of n_{sites} and of the parameters which characterize the distribution $P(\delta)$.

First let us take one flat distribution $P(\Delta_1)=P(\delta)=1/\delta_{max}$ for $\delta<\delta_{max}$, and $P(\delta)=0$ otherwise. This is one case where an analytical expression for n_{ads} exists:

$$n_{ads}=n_{sites}\frac{k_BT}{\delta_{max}}\frac{\ln[1-x+c(\delta_{max})x]}{1-x}\ .$$

We did not succeed in obtaining a good fit with only one flat distribution. But a reasonable agreement between the data and the model is obtained (see Fig. 3) when we use three distributions implying three sets of values of $(\delta^i_{max},n^i_{sites})$: $n_{ads}=\sum n^i_{ads}(n^i_{sit},\delta^i_{max}),i=1-3$. The values of the parameters are $\delta^1_{max}=37.15$ K, $n^1_{sites}=262$ μmol; $\delta^2_{max}=98.7$ K, $n^2_{sites}=243$ μmol; and $\delta^3_{max}=164.5$ K, $n^3_{sites}=99$ μmol. The solid curves represent the results of the fit. They are superimposed perfectly in this diagram on the experimental data, except for the low-temperature part of the data corresponding to $n_{tot}=164$ μmol (see the curve denoted a in Fig. 3). We find a total number of sites $n_{sites}=\Sigma n^i_{sites}$, which equals 604 μmol in our sample. In Fig. 4, we have plotted $n_{sites}P(\Delta_1)=\Sigma(n^i_{sites}/\delta^i_{max})$ vs Δ_1, which gives the total number of sites of binding energy Δ_1. The general shape of the distribution suggests that an exponential distribution $P(\Delta_1)\sim\exp(-\Delta_1/\delta_0)$ could fit the data rather well, involving only two parameters δ_0 and n_{sites}. In that case, we have no analytical solution for n_{ads} and we have to integrate $\bar{n}$ numerically over the distribution of Δ_1. We found $\delta_0=37.6\pm0.2$ K and a number of sites close to the previous one: $n_{sites}=677\pm4$ μmol, i.e., 10% larger than in the assumption of a three-stripe distribution. In Fig. 3, we have also plotted the experimental data together with the results of the latter fit. As previously, the experimental and calculated data cannot be distinguished, except here for the lowest curve, which corresponds to $n_{tot}=21.8$ μmol (see the curve denoted b in Fig. 3). This is the region where P_{meas} is very small and therefore less accurately measured. We show the corresponding distribution $n_{sites}P(\delta)$ in Fig. 4. The total number of sites yields to a specific area of our sample of the order of 180 m^2/cm^3 or 1100 m^2/g, in relative agreement with Ref. 11.

In Fig. 2(a) we present the result (solid line) of the best fit of the quantity n_{ads}/n_{tot}. Here again we fit all the data together to find the values of n_{sites} and of the parameters of the distribution $P(\delta)$. In that case, we directly calculate n_{ads}/n_{tot} from Eq. (5), where we use the experimental values $x_{expt}(T)$ for calculating n_{ads}. Here we suppose an exponential distribution of δ. We find values of δ_0 and of n_{sites} which are equal to those given by the previous fit of x_{expt}. We note a strong disagreement between the experimental and calculated data obtained at the smallest value of n_{tot} (see upper curve). In addition, the calculated data give values of n_{ads}/n_{tot} which are larger than unity. All this is due to the uncertainty about the value of the pressure, and therefore about x_{expt}, when P_{meas} is small, which is the case for small values of n_{tot}. Also, we find that the calculated values of n_{ads}/n_{tot} are larger than the experimental ones at high temperature. This can be attributed to the fact that we did not introduce any physical cutoff in the exponential distribution, which should avoid the overestimation of adsorbed atoms above 20 K.

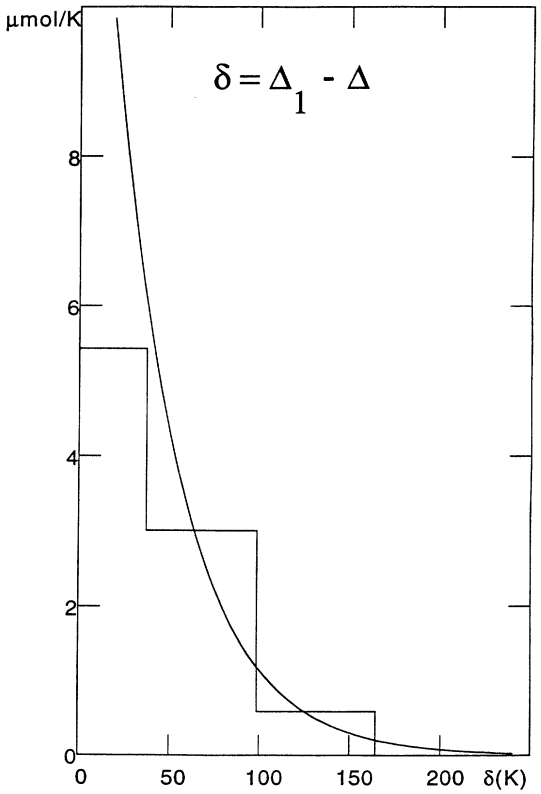

FIG. 4. The Δ_1 dependence of the number of sites of energy Δ_1 as given by the two distributions considered in the fits of Fig. 3.

IV. EXPANSION OF THE GEL

Through this study, which depends on the elasticity of the fractal structure, we have access to the elastic behavior corresponding to microscopic length scales. This behavior will then be compared to the macroscopic elasticity.

A. Experimental data

We have measured the length change of the sample simultaneously with the number of atoms adsorbed on the silica surface. In Fig. 5, we present the thermal expansion of dry aerogels of various density together with that of amorphous silica. For the aerogel of density 0.16 g/cm^3, we also show the expansion in the presence of He gas in the cell. One observes a large extra contribution to the expansion due to adsorption. It is this extra contribution that we show in Fig. 6 for different amounts of He introduced into the cell. These amounts n_{tot} are given in the legend of Fig. 6. For $n_{\text{tot}} > 3n_{\text{sites}}$, we observe a dilatation followed by a contraction of the sample (not shown for clarity in Fig. 6) when the temperature is lowered. We interpret this behavior as a progressive adsorption of helium when lowering T, followed by the formation of a liquid-He film on the silica surface: When the first layer is fully complete and does not contribute anymore to the expansion (see the following) the surface of the film has to contract in order to decrease its surface energy. The net result is a contraction of the gel.

B. Model of expansion induced by adsorption

We write the grand potential Ω as the sum of the surface contribution Ω_S due to adsorption, plus an elastic energy term for the gel which involves the macroscopic bulk modulus B:

$$\Omega=\Omega_S+\frac{BV}{2}\left[\frac{\delta V}{V}\right]^2 . \tag{7}$$

To obtain the extra expansion of the gel due to absorption, we have to minimize Ω with respect to all microscopic strains $\delta v_i/v_i$ of particles i and with respect to the volume V. We obtain

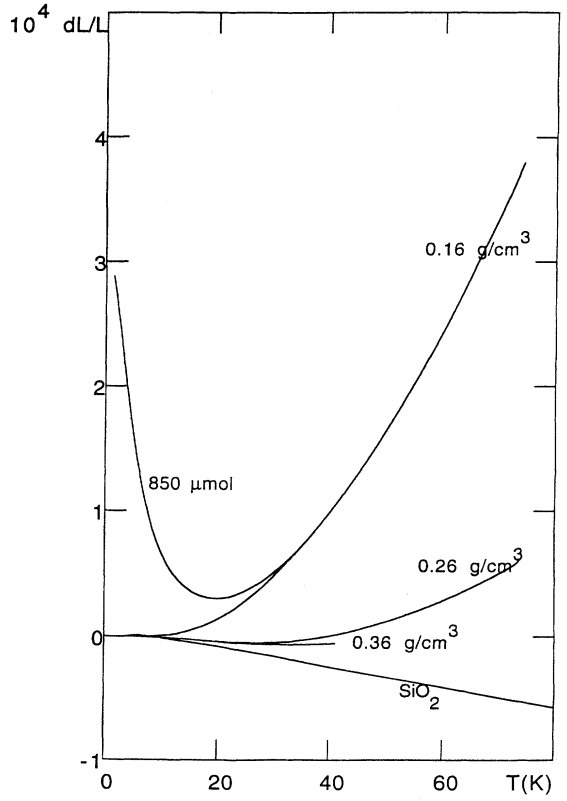

FIG. 5. Thermal expansion dL/L of some dry aerogels and of amorphous silica. The expansion of the aerogel of density $\rho=0.16$ g/cm^3 in the presence of gas introduced into the cell is also shown. The data reveal a large extra expansion due to adsorption.

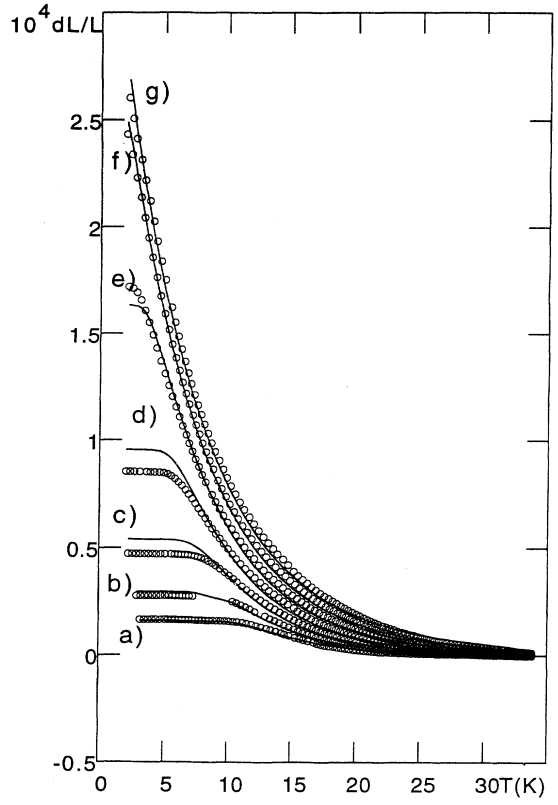

FIG. 6. The extra expansion dL/L due to adsorption is represented vs T for different amount n_{tot} of He gas: 21.94 μmol (a), 43.5 μmol (b), 85.44 μmol (c), 164.9 μmol (d), 307.7 μmol (e), 538.2 μmol (f), and 840.3 μmol (g). The points represent the experimental data, and the solid curves correspond to the calculated values of dL/L involving the exponential distribution of Fig. 4.

$$0=BV\frac{\delta V}{V}+\Sigma\left[\frac{V\partial v_i}{v_i\partial V}\right]\left[\frac{v_i\partial\Omega_S}{\partial v_i}\right]_{T,\mu} . \quad (8)$$

The derivative $\varepsilon=(V\partial vi/v_i\partial V)$ has the same meaning as in Sec. I, namely the change of v_i which minimizes the elastic energy for a given $\delta V/V$. Equation (8) can be written in the following form

$$\frac{\delta V}{V}=-\frac{2}{3}\left[\frac{\varepsilon}{BV}\right]\left[S\frac{\partial\Omega_S}{\partial S}\right]_{T,\mu} , \quad (9)$$

where the prefactor $\frac{2}{3}=v_i ds/s\, dv_i$ is the ratio of the relative change of surface of a particule to the change of its volume. We can interpret Eq. (9) as given by a simple minimization of Ω with respect to S from Eq. (7), but where the bulk modulus B measured under external stress has to be replaced by (B/ε) which is an elastic constant which counteracts the dilatation due to the Ω_S term. Now we focus on Ω_S. For a continuous surface, $\Omega_S=\gamma S$, where γ is the surface free energy. Thus[13]

$$\frac{\partial\Omega_S}{\partial S}=\gamma+S\frac{\partial\gamma}{\partial S} .$$

The difference between the surface free energy (γ) and the surface stress, also called the spreading pressure ($\partial\Omega_S/\partial S$), has been clearly illustrated on a variety of simple models in Ref. 14. Our derivation of (9) is based on a recent review[15] of the thermodynamics of solid-solid and solid-fluid interfaces.

To give a microscopic picture, we write Ω_S to be $\Omega_{/\text{site}}$ times the available number n_{sites} of sites of adsorption at the surface of silica. In Eq. (9), Ω_S is differentiated with respect to the real surface S,

$$\frac{\partial\Omega_S}{\partial S}=\Omega_{/\text{site}}\frac{\partial n_{\text{sites}}}{\partial S}+n_{\text{sites}}\frac{\partial\Omega_{/\text{site}}}{\partial S} .$$

Now we will interpret the first term. Since $\Omega_{/\text{site}}=-kT\ln(\xi)$ is negative, it gives a positive expansion [see Eq. (9)], and involves all the adsorbed atoms as expected. Let us assume that $(\partial\Omega_{/\text{site}}/\partial S)=0$. Then the expansion exists only if n_{sites} is not constant when S changes. Let us consider the two following cases.

(i) If a number n_{tot} of atoms much smaller than n_{sites} is introduced in the cell, the number $\bar{n}_1$ ($\approx\bar{n}$) of atoms in the first layer is small and saturates to $n_{\text{tot}}/n_{\text{sites}}$ at low enough temperature. In that case $\ln(\xi)=-\ln(1-\bar{n}_1)$ also saturates. This implies that $\Omega_{/\text{site}}=-kT\ln(\xi)$ is a pure entropic term. Then the number of sites has to increase in order to increase the entropy per He atom. We note that the expansion goes to zero when T is decreased down to zero and it equals kTn_{tot} in the limiting case where $n_{\text{tot}}\ll n_{\text{sites}}$.

(ii) If the number of atoms introduced in the cell is larger than the number of sites, the first layer is almost complete. To decrease the surface energy further, the surface expands to increase the number of sites. In that case $\Omega_{/\text{site}}$ does not vanish as T goes to zero.

In the following we assume that n_{sites} increases proportionally to the surface, i.e., $n_{\text{sites}}=S/\sigma$, where σ is an effective surface occupied by an adsorbed helium atom. Now we comment on the term $n_{\text{sites}}(\partial\Omega_{/\text{site}}/\partial S)$. $\Omega_{/\text{site}}$ depends on surface strain only via Δ_1. Thus $Sd\Omega_{/\text{site}}/dS=\Gamma_{\text{site}}\Delta_1(\partial\Omega_{/\text{site}}/\partial\Delta_1)$, where $\Gamma_{/\text{site}}=(S\partial\Delta_1/\Delta_1\partial S)$ is a Gruneisen-like prefactor which accounts for the change of the binding energy of a site associated with a deformation of the local surface. Since $(\partial\Omega_{\text{He}}/\partial\Delta_1)=-\bar{n}_1$, we obtain

$$\frac{dV}{V}=-\frac{2}{3}\frac{\varepsilon}{BV}n_{\text{sites}}\{\Omega_{/\text{site}}-\Gamma_{/\text{site}}\Delta_1\bar{n}_1\} . \quad (10)$$

Let us comment on the second term in the brackets. The energy $\Delta_1\sim\Sigma R_{ij}^{-6}$ is due to the contribution of the van der Waals interaction of one He atom (i) with all the atoms (j) of the surface and not only with one surface atom below it. Thus an expansion of the surface changes the distances R_{ij} and therefore Δ_1. This mechanism affects only the He atoms located on the surface, so it is normal to recover a dependence of the second term only on the number $\bar{n}_1$ of atoms adsorbed in the first layer. The importance of the second term on dV/V can be emphasized in the case of a small number n_{tot} of atoms introduced in the cell. When T goes to zero, it contributes to a finite value of dV/V because $(\Gamma_{/\text{site}}\Delta_1\bar{n}_1)$ remains finite while the first term in the brackets goes to zero as kTn_{tot}.

C. Quantitative fit

In the model presented above, we have actually considered the case of a flat surface involving a single value of Δ_1. For a broad distribution of Δ_1, most of the previous results apply and we have to integrate dV/V given by Eq. (10) over the distribution $P(\Delta_1)$ of the binding energies for $0<\delta=(\Delta_1-\Delta)<\delta_{\max}$. At this step we want to make a remark and to stress a difficulty, both coming from the distribution of Δ_1. The remark concerns the behavior of the expansion for a small number n_{tot} of atoms introduced in the cell. Indeed, when T is decreased from high temperatures, atoms concentrate in the regions of large Δ_1, and other atoms continue progressively to absorbate in the same regions. In these regions, we are in case (ii) previously discussed, so the first term of dV/V should not vanish as kTn_{tot} in contrast with the case of a single Δ_1 value. The difficulty arises for the integration of dV/V because $\Gamma_{/\text{site}}$ should depend on δ. Indeed the value of Δ_1 is linked to the distribution of distances R_{ij} of an adsorbed atom (i) to the surface atoms (j) in the neighborhood. So the distribution of Δ_1 is due to the distribution of the local curvatures of the surface . When the radius of the curvature is small and positive (a spike at the surface), Δ_1 should be small, while when this radius is small but negative (a hole), Δ_1 should be large. The expansion of the surface changes the values of R_{ij}. We can think intuitively that the expansion should increase Δ_1 in the case of a spike: the term $\Gamma_{/\text{site}}=\partial\ln\Delta_1/\partial\ln S$ is positive and favors the expansion. In contrast, the expansion should decrease Δ_1 in the case of a hole or of a flat surface: $\Gamma_{/\text{site}}$ is negative and counteracts the expansion. Consequently the value of $\Gamma_{/\text{site}}$ is a function of Δ_1, the sign of which depends on the range

of values of Δ_1. Since we do not have a precise model to describe the $\Gamma(\Delta_1)$ variation, we set it as a constant in the integration of Eq. (10) over $P(\delta)$. This is the main limitation of our calculation of dV/V.

In general, no simple relation between dV/V and the number n_{ads} of adsorbed atoms exists. Even in the case of an exponential distribution $P(\delta)$, for which we find the first term of dV/V proportional to n_{ads} for small x, the Γ term involves an integration of $\bar{n}_1$ over $\delta P(\delta)$ which cannot give a simple function of n_{ads}. We fit all our expansion data altogether to find the values of ε and Γ which are presented in Table I. We use the distributions determined in Sec. III, with the same values of the parameters, i.e., the number of sites and the distribution width. The agreement is very reasonable as shown in Fig. 6, where the solid curves represent the result of the best fit for the previous exponential distribution. The agreement is equally good when we use the previous set of three flat distributions. In the case of the exponential distribution the calculated value of dL/L is larger than the experimental one at high temperature. This is probably due to the fact that we did not put any cutoff at large values of Δ_1 in the exponential leading to an overestimation of dL/L above 20 K (see Fig. 7). Actually a maximum value of Δ_1 should exist corresponding to a hole in the surface. In the case of the three-stripe distribution, we find a negative value of $\Gamma_{/sites}$ for the stripe of largest $\Delta_{1\,max}$, while it is positive for the other stripes. This result is in agreement with our intuition about the sign of Γ, as discussed above.

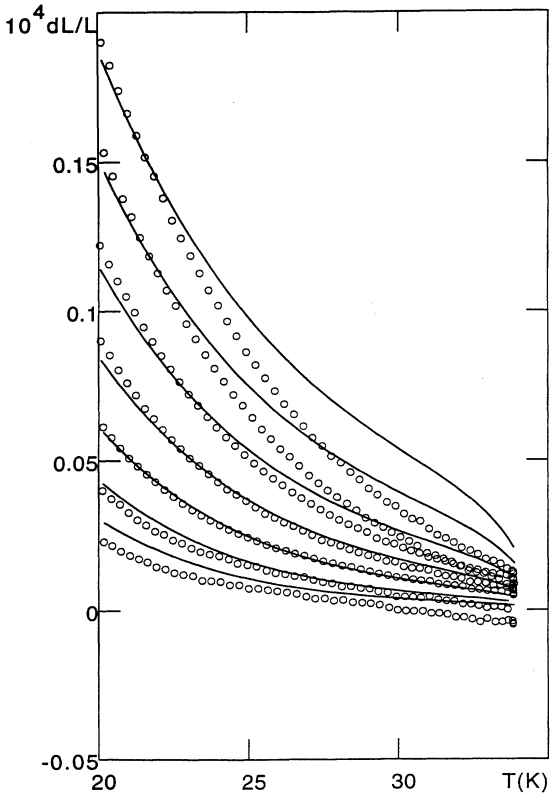

FIG. 7. The expanded view of Fig. 6 above 20 K shows that the absence of a cutoff in the exponential distribution of the binding energy leads to an overestimation of the calculated dilatation in this range.

TABLE I. The values of the parameters Γ and ε (see text), deduced from expansion measurements, taking $B = 60$ bar. The values are listed for the three-stripe model and the exponential distribution.

Three stripes δ_{max} (K)	n_{sites} (μmol)	Γ	$2\varepsilon/3$
37.15	262	3.2	7×10^{-4}
98.72	243	0.24	4.5×10^{-3}
164.5	99	-1	-2×10^{-3}
Exponential δ_0 (K)			
37.6	677	0.125	3×10^{-3}

In order to deduce the value of ε one needs to estimate the bulk modulus B. No data for B exist, since it is impossible to apply a hydrostatic pressure on an aerogel. Nevertheless the value of B is related to the Young modulus E: $B = E/3(1-2\sigma)$, where σ is the Poisson ratio which is known to be generally positive and of maximum value $\frac{1}{2}$ in the case of liquids. In amorphous silica one finds $B = E/2$. We can also take a reasonable value of σ: $\sigma \approx \frac{1}{3}$, i.e., $B \approx E$. Using these values, we obtain an order of magnitude for ε of about 10^{-3}, i.e., the order of magnitude that we gave in Sec. I. The significance of this is that, when a macroscopic stress is imposed, the contribution to the deformation from compression of the particles is 10^3 times smaller than that from the bending of the microrods which compose the porous medium.

V. CONCLUSION

To be able to describe the absorption data of He on an aerogel we have assumed a broad distribution $P(\Delta_1)$ of the binding energies. We have shown that $P(\Delta_1)$ has to be a decreasing function of Δ_1 such as those given in Fig. 4. We could recover the observed expansion behavior by using a simple model where the calculation of the change of surface tension in the presence of adsorption is made with the same distribution $P(\Delta_1)$ found from the adsorption analysis. We have estimated the value of the geometrical factor ε which relates the deformation at microscopic scales to that at macroscopic scales.

ACKNOWLEDGMENTS

We are very grateful to the Montpellier group M. Leverrier-Forêt, T. Woignier, J. Pelous, and R. Vacher for providing the aerogels samples. A. Forbes and S. Fisher are acknowledged for critical readings of the manuscript.

APPENDIX: SERIES EXPANSION FOR Ω

Our starting point is the grand partition function for one site at fixed δ: $\xi=1+Cx/1-x$, where $x=\exp[\beta(\mu+\Delta)]$. From ξ we can calculate the grand potential $\Omega=-k_BT\ln\xi$, and $\bar{n}=x\partial\xi/\xi\partial x$.

(a) In the above expressions, $z=x/1-x$ appears like an effective fugacity for a Langmuir isotherm (for which only the first layer exists). The complication of introducing the next layers is thus so slight that we consider it worthwhile to track this extra factor. (b) The Langmuir isotherm $\xi=1+C\alpha$ is identical to the Fermi-Dirac distribution, and the expansions given below are closely related to the Sommerfeld expansion for the chemical potential of an electron gas.

In the following we consider a distribution $dN=P(\delta)d\delta$ of adsorption energies. We have explicitly chosen distributions with only one energy scale δ_M, and we focus on two cases: (1) stripe: $P(\delta)=1/\delta_M$ for $0<\delta<\delta_M$; and (2) exponential tail: $P(\delta)=(1/\delta_M)\exp(-\delta/\delta_M)$. Although for the stripe $\bar{n}$ can be calculated analytically, this is not the case for Ω. For the exponential neither quantity can be calculated exactly. The purpose of the appendix is to obtain these quantities as series expansion in $u=Cz$ and $D=k_BT/\delta_M$, where $C=\exp(\beta\delta)$ and $C_M=\exp(\beta\delta_M)$.

1. Calculation for the stripe

$-\Omega/k_BT=D\{I(u_M)-I(u_m)\}$ where $u_m=z$, $u_M=C_Mz$, and $I(\alpha)=\int_1^\alpha(du/u)\ln(1+u)$. In $I(\alpha)$ the logarithm can be expanded in powers of u, provided that $u<1$. In the case where $\alpha>1$ we use the identity $I(\alpha)=(\ln\alpha)^2/2-I(1/\alpha)$, so that the expansion

$$I(\alpha)=\sum_{n>0}\frac{(-)^n}{n^2}(1-\alpha^n) \tag{A1}$$

allows us to obtain Ω for any α. A similar expression is used for calculating $\delta_M\partial\Omega/\partial\delta_M$, needed for the surface stress.

2. Calculation for the exponential

We preferred in that case to use the cumulated distribution $N(\delta)=\int_\delta^\infty P(\Delta)d\Delta=\exp(-\delta/\delta_M)$, and to integrate by parts:

$$-\frac{\Omega}{k_BT}=[N(\delta)\ln(1+C\alpha)]_{\delta=0}^{\delta=\infty}+\int\frac{zdC}{1+Cz}\exp(-\delta/\delta_M)$$

$$=\ln(1-x)-z^D\int_z^\infty\frac{du}{u^D(1+u)}\ . \tag{A2}$$

We thus use (for $z<1$) the quantity

$$I(D,z)=\int_z^1\frac{du}{u^D(1+u)}=\sum_{n\geq0}\frac{(-)^n}{n+1-D}(1-z^{n+1-D})\ . \tag{A3}$$

In (A2) the part of the integral for $z>1$ is converted to $I(1-D,0)$. Our final expression is $-\Omega/k_BT=-\ln(1-x)+z^D\{I(D,z)+I(1-D,0)\}$.

Series (A3) converges for any $z<1$ and D. Concerning our experiments z is always significantly less than 1, and we replaced $I(D,z)$ by $I(D,0)$. This amounts to having an uncut exponential tail of nonbinding sites, whose total number is infinite. Of course this expansion then diverges for $D\geq1$. Although the exact series could be used, in our experiment we checked that z could be effectively neglected in $I(D,z)$. The code needed for adjusting the model to the data described below is then much more efficient since, for a given D, the curly bracketed term has to be calculated only once for all the values of z. Similar expressions are used for calculating $\delta_M\partial\Omega/\partial\delta_M$ and $\bar{n}$.

3. Procedures for adjusting the model(s) to the data

The quantities P, $n_{\rm ads}/n_{\rm tot}$, and dL/L have been fitted to the model and different methods have been used for that purpose. In each case the parameter(s) of the model are adjusted so as to minimize the correctly defined χ^2, taking into account the error bars on the fitted quantity. This adjustment is performed with an algorithm based on that of Levenberg and Marquardt.[16] The major improvement made on that algorithm is to consider separately the parameters which enter linearly into the model, and those that enter nonlinearly.

Concerning the pressure, two adjustments have been made. The most straightforward method uses the measured pressure for evaluating x. The number of adsorbed atoms is then linear in $n_{\rm site:}(n_{\rm ads}/n_{\rm tot})=(n_{\rm site}/n_{\rm tot})\bar{n}(x,D)=1-P/P_{\rm calc.}$ Thus $n_{\rm site}$ is found by linear regression of $1-P/P_{\rm calc}$ versus $\bar{n}(x,D)$. Generalization of this to many stripes (e.g., three) is straightforward.

The major drawback of this method is that the measured pressure enters both into the fitted quantity and into the fitting function $\bar{n}(x,D)$. The latter function in turn varies extremely rapidly with P at low pressure, so that a large error bar on the fitting function exists.

The second method differs in that respect. For fixed parameters of the models (δ_M's and $n_{\rm site}$'s) we numerically solve the equation $x=x_{\rm eff}\,[1-\sum(n_{\rm site}/n_{\rm tot})\bar{n}(x,D)]$, where $x_{\rm eff}$ is the value of x if no atoms are adsorbed. That value of x is then compared to the measured one.

Finally, for comparing dL/L with our model, the numbers δ_M(s) and $n_{\rm site}$(s) were fixed to the values determined by the pressure. dL/L is then linearly adjusted to the basis of functions Ω and $\delta_M\partial\Omega/\partial\delta_M$, x being determined by the method described above (i.e., not using the measured pressure).

Let us finally note that the adjustment of dL/L to the model can be performed without any reference to pressure measurements. The problem in that case is that the number of parameters is so large that convergence of a minimization procedure is not guaranteed. For our results, the quality of the fit obtained in that way is slightly better than that using δ_M and $n_{\rm site}$ obtained from the pressure measurements, but the value of the physical parameters (δ_M, $n_{\rm site}$, ε) are not significantly altered.

[1]D. C. J. Yates, Proc. R. Soc. London Ser. A **224**, 526 (1954).
[2]F. T. Meeham, Proc. R. Soc. London **1555**, 199 (1927).
[3]D. Bellet and G. Dolino, Phys. Rev. B **50**, 17 162 (1994).
[4]T. Woignier, J. Phalippou, R. Sempere, and J. Pelous, J. Phys. (Paris) **49**, 289 (1988).
[5]G. Deutscher, R. Maynard, and O. Parodi, Europhys. Lett. **6**, 49 (1988).
[6]A. M. De Goer, R. Calemczuk, B. Salce, J. Bon, E. Bonjour, and R. Maynard, Phys. Rev. B **40**, 8327 (1989).
[7]The samples are prepared following the method described in R. Vacher, T. Woignier, J. Pelous, and E. Courtens, Phys. Rev. B **37**, 6500 (1988).
[8]The bridge is built by the company Barras-Provence under license of CRTBT-CNRS.
[9]F. R. Kroeger and C. A. Swenson, J. Appl. Phys. **48**, 853 (1977).
[10]R. A. Watkins, W. L. Taylor, and W. J. Haubach, J. Chem. Phys. **46**, 1007 (1967).
[11]G. Schuck and W. Dietrich, in *Aerogels: Proceedings of the First International Symposium,* edited by J. Fricke (Springer-Verlag, Berlin, 1986), p. 148.
[12]S. Brunauer, P. H. Emmett, and E. Teller, J. Am. Chem. Soc. **60**, 309 (1938).
[13]Here we recognize the Shuttleworth relation $\Pi_{\perp}=\gamma+S(\partial\gamma/\partial S)$, where $\Pi_{\perp}$ is the surface stress; see R. Shuttleworth, Proc. Phys. Soc. A **63**, 444 (1949).
[14]J. G. Dash, J. Suzanne, H. Shechter, and R. E. Peierls, Surf. Sci. **72**, 219 (1978).
[15]Ph. Nozières, in *Solids Far from Equilibrium,* edited by C. Godreche (Cambridge University Press, London, 1992), p. 1.
[16]D. W. Marcquardt, J. Soc. Ind. Appl. Math. **11**, 431 (1963); W. H. Press *et al.*, *Numerical Recipes* (Cambridge University Press, London, 1992).